

VISUALIZATION OF THE BIFURCATION LOCUS OF CUBIC POLYNOMIAL FAMILY

HIROYUKI INOU

ABSTRACT. Recent computers are getting fast enough to compute some dynamical or fractal objects in complex two-dimensional space. We show some attempts to visualize bifurcation locus of two-dimensional parameter space for complex dynamics in one variable by computer.

1. INTRODUCTION

Computer pictures of fractal objects such as the Mandelbrot set and Julia sets by numerical computation plays quite an important role to give deep insights in the study of complex dynamics. One can easily see that there are a lot of baby Mandelbrot sets (homeomorphic copies of the Mandelbrot set in itself), the Julia sets and filled Julia sets moves discontinuously, and many other phenomena.

Computers can numerically compute forward orbits quite fast (and backward orbits for low degree cases), and complex one-dimensional objects fit well with computer monitor. However, for higher-dimensional objects, although we can still compute orbits easily, it becomes very difficult to visualize such an object.

One simplest way for visualization is taking a projection. But to project an object in a higher dimensional space to a lower dimensional space, the object must be sparse. For example, for complex one-dimensional object, it is often the case to put a color on every pixel in the view. However, it is impossible to see such an object in complex two-dimensional space by projecting real three or two-dimensional space. Therefore, it is also necessary to develop algorithms to calculate sparse objects; the following are examples of such sparse objects:

- **For two-dimensional complex dynamical systems** (such as Hénon maps): Second Julia sets or (the closure of) the set of saddle or repelling periodic points are analogues of Julia set for one-dimensional dynamics and look sparse in many cases. Also, stable and unstable manifolds for a saddle have complex one-dimensional, hence it might be possible to see them by projecting to \mathbb{R}^3 .
- **For two-dimensional parameter space for one-dimensional dynamics** (such as the cubic polynomial family and the quadratic rational family): The support of the bifurcation measure or (the closure of) the set of Misiurewicz parameters are ones of the most sparse analogues of the boundary of the Mandelbrot set. As an analogue of (un)stable manifolds in higher-dimensional phase spaces, one can consider one-parameter spaces and the bifurcation loci in them.

In the past few years, Ushiki has been producing many pictures and movies of complex two-dimensional Julia sets using his program *Stereo Viewer* [U] which runs

on Mac OS X (recent versions seem to work only on Intel Macs). Stereo Viewer uses Biham-Wenzel's method [DMS] to numerically find a lot of periodic points, which is mathematically wrong in general, but seems to work very well. Then it projects those points to \mathbb{R}^3 and displays using OpenGL library. Recently, one can also see stable and unstable manifolds of saddle fixed points together with those periodic points.

Here, we consider some complex two-dimensional parameter spaces of one-dimensional dynamics, mainly the simplest one; the family of cubic polynomials. We explain how to calculate numerically fractal objects in the cubic polynomial family for visualization by Stereo Viewer and show some pictures we have obtained.

In parameter spaces, natural objects corresponding to (repelling or saddle) periodic points are *Misiurewicz maps*. For the family of polynomials of given degree, Dujardin and Favre proved that the support of the bifurcation measure coincides with the closure of the Misiurewicz parameters [DF]. Thus instead of the Biham-Wenzel's method, we use their landing theorem to calculate the bifurcation measure.

This is a very first attempt to see complex two-dimensional parameter space somewhat directly, hence the pictures are clearly not enough to see various phenomena. We also discuss what prevents from making finer pictures. We also discuss further possible improvements to refine those pictures.

Acknowledgment. The author would like to express his gratitude to Shigehiro Ushiki for explaining the usage of Stereo Viewer and helpful comments. He would also thank William Thurston for variable suggestions.

2. FAMILY OF CUBIC POLYNOMIALS

For $(a, b) \in \mathbb{C}^2$, we consider the following family of cubic polynomials:

$$f_{a,b}(z) = z^3 - 3a^2z + b.$$

This family is considered as the family of affine conjugacy class of cubic polynomials with the following two markings:

- *Critical marking:* the critical point $+a$ is considered as the *marked* (or first) critical point and $-a$ is the other (or second) critical point of $f_{a,b}$.
- *Böttcher marking:* since $f_{a,b}$ is monic, it has the Böttcher coordinate $\varphi_{a,b}$ of $f_{a,b}$ at infinity, i.e., a conformal map defined near infinity such that

$$(1) \quad \varphi_{a,b}(f_{a,b}(z)) = (\varphi_{a,b}(z))^3$$

and $\varphi_{a,b}$ is asymptotic to the identity ($\lim_{z \rightarrow \infty} \frac{\varphi_{a,b}(z)}{z} = 1$).

More precisely, for any triple (f, ω, φ) of a cubic polynomial, a critical point and a Böttcher coordinate for f (without the asymptotic condition at infinity), there exists a unique $(a, b) \in \mathbb{C}^2$ and an affine map $A : \mathbb{C} \rightarrow \mathbb{C}$ such that

$$f_{a,b} = A \circ f \circ A^{-1}, \quad A(\omega) = a, \quad \varphi_{a,b} \circ A = \varphi.$$

There are two natural involutions $\iota_{\text{can}} : \mathbb{C}^2 \rightarrow \mathbb{C}^2$ and $\iota_{\text{cp}} : \mathbb{C}^2 \rightarrow \mathbb{C}^2$ as follows:

- The canonical involution $\iota_{\text{can}}(a, b) = (-a, -b)$ is given by the conjugacy $-f_{a,b}(-z) = f_{-a,-b}(z)$.
- $\iota_{\text{cp}}(a, b) = (-a, b)$ preserves the dynamics and swaps the role of two critical points of $f_{a,b}$.

Simply as a cubic polynomial (without any marking), four maps $f_{\pm a, \pm b}$ are affinely conjugate in general.

For $(a, b) \in \mathbb{C}^2$, let us denote the filled Julia set and the Julia set for $f_{a,b}$ as follows:

$$\begin{aligned} K_{a,b} &= \{z \in \mathbb{C}; \{f_{a,b}^n(z)\}_{n \geq 0} \text{ is bounded}\}, \\ J_{a,b} &= \partial K_{a,b}. \end{aligned}$$

It is well-known that $K_{a,b}$ (equivalently, $J_{a,b}$) is connected if and only if both of the critical points $\pm a$ are contained in $K_{a,b}$. Let us denote

$$\begin{aligned} \mathcal{C} &= \{(a, b); K_{a,b} \text{ is connected}\} = \{(a, b); +a, -a \in K_{a,b}\} \\ \mathcal{S} &= \{(a, b); +a, -a \in \mathbb{C} \setminus K_{a,b}\}. \end{aligned}$$

We call \mathcal{C} the *connectedness locus* and \mathcal{S} the *shift locus*.

We say a map $f_{a,b}$ is *Misiurewicz* if both of the critical points $\pm a$ are strictly preperiodic. We denote the set of all Misiurewicz parameters by Mis .

The Böttcher coordinate $\varphi_{a,b}$ defines *external rays* for $f_{a,b}$: First assume the filled Julia set is connected. Then $\varphi_{a,b}$ can be extended to a conformal map $\varphi_{a,b} : \mathbb{C} \setminus K_{a,b} \rightarrow \mathbb{C} \setminus \bar{\mathbb{D}}$ by the functional equation (1), where $\mathbb{D} = \{|z| < 1\}$ is the unit disk. The *external ray* of angle $\theta \in \mathbb{R}/\mathbb{Z}$ for $f_{a,b}$ is defined by

$$R_{a,b}(\theta) = \varphi_{a,b}^{-1}\{\exp(r + 2\pi i\theta); r \in (0, \infty)\}.$$

If $K_{a,b}$ is not connected, then $\varphi_{a,b}$ cannot be defined on the whole of $\mathbb{C} \setminus K_{a,b}$. However it is known that $R_{a,b}(\theta)$ can still be defined unless it ‘‘bifurcates’’ at a backward image of escaping critical points (see figure 1). In particular, if at least one of the critical points $\pm a$ escapes to infinity, there are always two or more rays which bifurcates at the critical point for the first time.

By the functional equation (1), we have

$$(2) \quad f_{a,b}(R_{a,b}(\theta)) = R_{a,b}(3\theta).$$

The *Green’s function* $g_{a,b} : \mathbb{C} \rightarrow [0, \infty)$ for $f_{a,b}$ is defined as follows:

$$g_{a,b}(z) = \lim_{n \rightarrow \infty} \frac{1}{3^n} \log^+ |f_{a,b}^n(z)|,$$

where $\log^+(x) = \max\{\log(x), 0\}$. The set

$$E_{a,b}(r) = \{g_{a,b}(z) = r\}$$

for $r > 0$ is called the *equipotential curve* of potential r for $f_{a,b}$. The Green’s function and the Böttcher coordinate satisfy the following equations:

$$\begin{aligned} g_{a,b}(f_{a,b}(z)) &= 3g_{a,b}(z), \\ \log |\varphi_{a,b}(z)| &= g_{a,b}(f_{a,b}(z)), \text{ if } \varphi_{a,b}(z) \text{ is defined.} \end{aligned}$$

3. BIFURCATION MEASURE

In this section, we describe the definition of the bifurcation measure and the landing theorem by Dujardin and Favre [DF].

The landing theorem states that the bifurcation measure is the image by the ‘‘landing map’’ $e : \text{Cb} \rightarrow \mathcal{C}$ of the natural measure of the combinatorial space Cb .

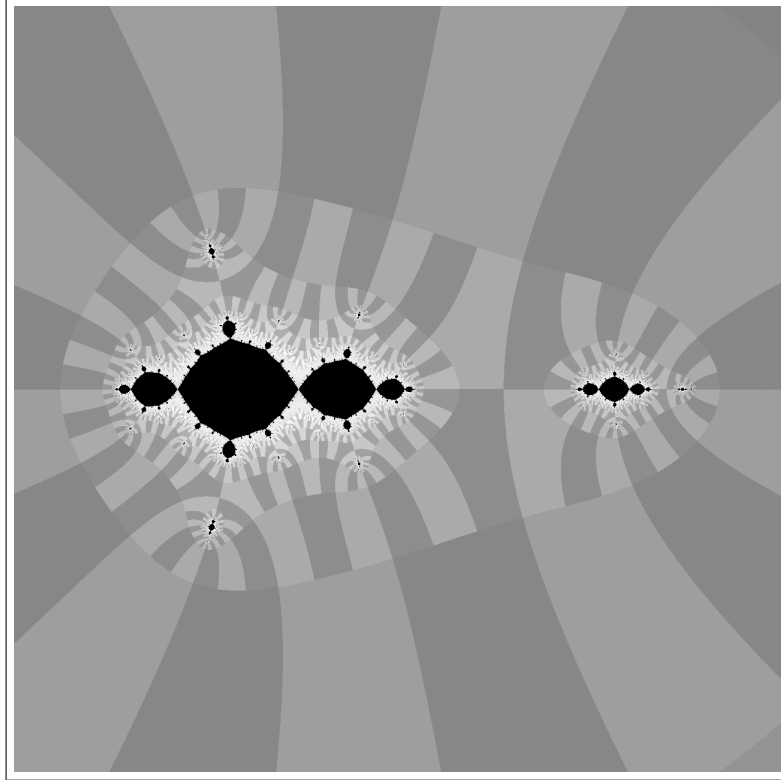


FIGURE 1. The external rays of angle $1/6$ and $5/6$ bifurcate at the escaping critical point. Backward images of those rays also bifurcate.

3.1. Critical portrait and combinatorial space. We describe the combinatorial space only for cubic polynomials. See [DF] for more details.

For simplicity, we only consider the case $f_{a,b} \in \mathcal{S}$ and

$$(3) \quad g_{a,b}(a) = g_{a,b}(-a) = r$$

for some $r > 0$. Let $\Theta^\pm = \Theta_{a,b}^\pm$ be the set of external angles for $\pm a$, i.e., the set of $\theta \in \mathbb{R}/\mathbb{Z}$ such that $\overline{R_{a,b}(\theta)}$ contains (in fact, bifurcates at) $\pm a$. Since $f_{a,b}(\pm a)$ has potential $3r > r$, there exists a unique external ray $R_{a,b}(\eta^\pm)$ for some η^\pm . Then by (2), for any $\theta \in \Theta^\pm$, we have $3\theta = \eta^\pm$. It implies that the cardinality of Θ^\pm is two if $\pm a$ is a simple critical point, and three if $\pm a$ is double (equivalently, $a = 0$). Therefore, we have exactly one of the following:

Non-degenerate case ($a \neq 0$): $\#\Theta^\pm = 2$ and they are unlinked.

Degenerate case ($a = 0$): $\Theta^+ = \Theta^-$, and $\#\Theta^+ = 3$.

We say two sets $A, B \subset \mathbb{R}/\mathbb{Z}$ are *unlinked* if B is contained in a component of $\mathbb{R}/\mathbb{Z} \setminus A$ (equivalently, vice versa).

The pair $\Theta = (\Theta^+, \Theta^-)$ is called the *critical portrait* of $f_{a,b}$. The *combinatorial space* Cb is the set of possible critical portraits for such $f_{a,b}$:

$$\text{Cb} = \{(\Theta_{a,b}^+, \Theta_{a,b}^-); (a, b) \in \mathcal{S} \text{ satisfying (3)}\},$$

And let Cb_0 be the set of critical portraits for non-degenerate $f_{a,b}$:

$$\text{Cb}_0 = \{(\Theta_{a,b}^+, \Theta_{a,b}^-) \in \text{Cb}; a \neq 0\}.$$

To describe the combinatorial space Cb in more understandable way, we introduce the notion of *cocritical points*, which are the points having the same image as the critical points. For $f_{a,b}$, we have $f_{a,b}(\mp 2a) = \mp 2a^3 + b = f_{a,b}(\pm a)$, hence the cocritical points are $\mp 2a$.

Now consider the non-degenerate case. Then there exists a unique external angle θ^\pm of $\mp 2a$ for $f_{a,b}$. Then it follows that $3\theta^\pm = \eta^\pm$ and $m_3^{-1}(\eta^\pm) = \Theta^\pm \cup \{\theta^\pm\}$, where $m_3 : \mathbb{R}/\mathbb{Z} \rightarrow \mathbb{R}/\mathbb{Z}$ is the three-fold covering map $m_3(t) = 3t$.

Then $\mathbb{R}/\mathbb{Z} \setminus \Theta^+$ has two components; say A and B and we may assume $\theta^+ \in A$. Then A has length $2/3$ and B has length $1/3$. Since Θ^- is contained in one of A and B and the two angles $\alpha_1^-, \alpha_2^- \in \Theta^-$ differs by $1/3$, the only possibility is $\Theta^- \subset A$. Hence it follows that $\theta^- \in B$. In other words, we have $\theta^- \in (\theta^+ + \frac{1}{3}, \theta^+ + \frac{2}{3})$.

It is known that one can define critical portrait combinatorially and all such combinatorially defined critical portrait can be realized as the one of some polynomial [G, Proposition 3.8]. In particular, we have a natural bijection

$$\text{Cb}_0 \rightarrow \{(\theta^+, \theta^-); \theta^- \in (\theta^+ + \frac{1}{3}, \theta^+ + \frac{2}{3})\} \subset (\mathbb{R}/\mathbb{Z})^2.$$

We identify Cb_0 and its image by this bijection. Let μ_{Cb} be the restriction of the Lebesgue measure on $(\mathbb{R}/\mathbb{Z})^2$ to Cb_0 , normalized such that $\mu_{\text{Cb}}(\text{Cb}_0) = 1$. We consider μ_{Cb} as a measure on Cb , i.e., extend μ_{Cb} by $\mu_{\text{Cb}}(A) = \mu_{\text{Cb}}(A \cap \text{Cb}_0)$.

Remark 3.1. In fact, $\text{Cb} \setminus \text{Cb}_0$ corresponds to critical portraits of the form $\Theta = \{\theta, \theta + \frac{1}{3}, \theta + \frac{2}{3}\}$ for some $\theta \in \mathbb{R}/\mathbb{Z}$. Hence Cb can be identified with

$$\{(\theta^+, \theta^-); \theta^- \in [\theta^+ + \frac{1}{3}, \theta^+ + \frac{2}{3}]\} / \sim$$

where $(\theta^+, \theta^-) \sim (\eta^+, \eta^-)$ if $\theta^-, \eta^+, \eta^- \in \theta^+ + \frac{1}{3}\mathbb{Z}$.

Goldberg's realization theorem [G, Proposition 3.8] allows us to define the following *Goldberg map* (see [DF, Proposition 7.12, 7.19]):

Theorem 3.2. *There exists a unique continuous map $\Phi_g : \text{Cb} \times (0, \infty) \rightarrow \mathcal{S}$ such that when $\Phi_g(\Theta, r) = (a, b)$, the following hold:*

- (1) $g_{a,b}(\pm a) = r$,
- (2) *the critical portrait of $f_{a,b}$ is Θ .*
- (3) $\Phi_g(\cdot, r)$ *is a homeomorphism from Cb onto $\mathcal{G}(r) = \{(a, b); g_{a,b}(\pm a) = r\}$.*
- (4) $e(\Theta) = \lim_{r \searrow 0} \Phi_g(\Theta)$ *exists for μ_{Cb} -almost every $\Theta \in \text{Cb}$.*

A measurable map $e : \text{Cb} \rightarrow \mathcal{C}$ is called the *landing map*.

Remark 3.3. The set

$$\{\Phi_g(\Theta, r); r \in (0, \infty)\}$$

is an example of *stretching rays*, introduced by Branner and Hubbard [BH].

Stretching rays are generalization of external rays for the Mandelbrot set. It is conjectured that the Mandelbrot set is locally connected. Hence, by Carathéodory's theorem, all external rays conjecturally land. On the contrary, Komori and Nakane [KN] proved that there exist stretching rays such that the accumulation set as $r \searrow 0$ is non-trivial; namely, such stretching rays do not land.

3.2. Bifurcation measure and landing theorem. The bifurcation measure μ_{bif} is first defined by Bassanelli and Berteloot, in terms of *bifurcation current*, which is introduced by DeMarco [DM]. Here we briefly recall the definition and state the landing theorem. See [DF, Section 6] for more details.

Let $G_{\pm}(a, b) = g_{a,b}(\pm a)$. Since $g_{a,b}$ is a subharmonic function, G_+ and G_- are plurisubharmonic functions on \mathbb{C}^2 . Hence we can consider $(1, 1)$ -currents

$$T_{\pm} = dd^c G_{\pm}.$$

A current defined by $T_{\text{bif}} = \frac{1}{2}(T_+ + T_-)$ is called the *bifurcation current* and $\mu_{\text{bif}} = T_+ \wedge T_- = \frac{1}{2}T_{\text{bif}} \wedge T_{\text{bif}}$ is a well-defined positive measure. We call μ_{bif} the *bifurcation measure*. Its support is equal to the Shilov boundary of \mathcal{C} , and also equal to the closure of Misiurewicz parameters $\overline{\text{Mis}}$ [DF, Corollary 6, Theorem 9].

The landing theorem [DF, Theorem 8] states the relationship between μ_{bif} and μ_{Cb} :

Theorem 3.4 (Landing theorem). $\mu_{\text{bif}} = e_* \mu_{\text{Cb}}$.

We explain how to numerically compute μ_{bif} in Section 5.2.

4. SUPERATTRACTING CURVES

For $p > 0$, let

$$\mathcal{S}_p = \{(a, b); f_{a,b}^n(a) \neq a \ (1 < n < p), f_{a,b}^p(a) = a\}$$

be the family of cubic polynomials whose marked periodic points have exact period p . It is called the *period p superattracting curve*.

Example 4.1. Case $p = 1$: Direct calculation shows that $\mathcal{S}_1 = \{(a, b); b = 2a^3 + a\}$, which is isomorphic to \mathbb{C} .

Case $p = 2$: Let $f_{a,b} \in \mathcal{S}_2$. By an affine change of coordinate, we may assume the marked critical point is 0 and its forward orbit is

$$0 \mapsto 1 \mapsto 0.$$

Then it has the form

$$\tilde{f}_t(z) = tz^3 - (t+1)z^2 + 1$$

for some $t \in \mathbb{C}^* = \mathbb{C} \setminus \{0\}$. The free critical point for \tilde{f}_t is $\frac{2(t+1)}{3t}$.

To take an affine conjugacy of \tilde{f}_t to a monic polynomial, we need to take a square root of t (the leading coefficient). Therefore, to embed \tilde{f}_t to (a, b) -plane, we put $t = s^2$ and parametrize \tilde{f}_t by s . Then \tilde{f}_{s^2} is affinely conjugate to $f_{a,b}$, where

$$(a, b) = \left(\frac{s^2 + 1}{3s}, -\frac{(s^2 - 2)(2s^4 - is^2 - 1)}{27s^3} \right).$$

Therefore, $\mathcal{S}_2 \cong \mathbb{C}^*$.

Case $p = 3$: Similarly, any $f_{a,b} \in \mathcal{S}_3$ is affine conjugate to a polynomial of the form

$$\hat{f}_{\alpha,\beta}(z) = \alpha z^3 + \beta z^2 + 1$$

with

$$\alpha = -\frac{c^3 - c^2 + 1}{c^3 - c^2}, \quad \beta = \frac{c^4 - c^3 + 1}{c^3 - c^2},$$

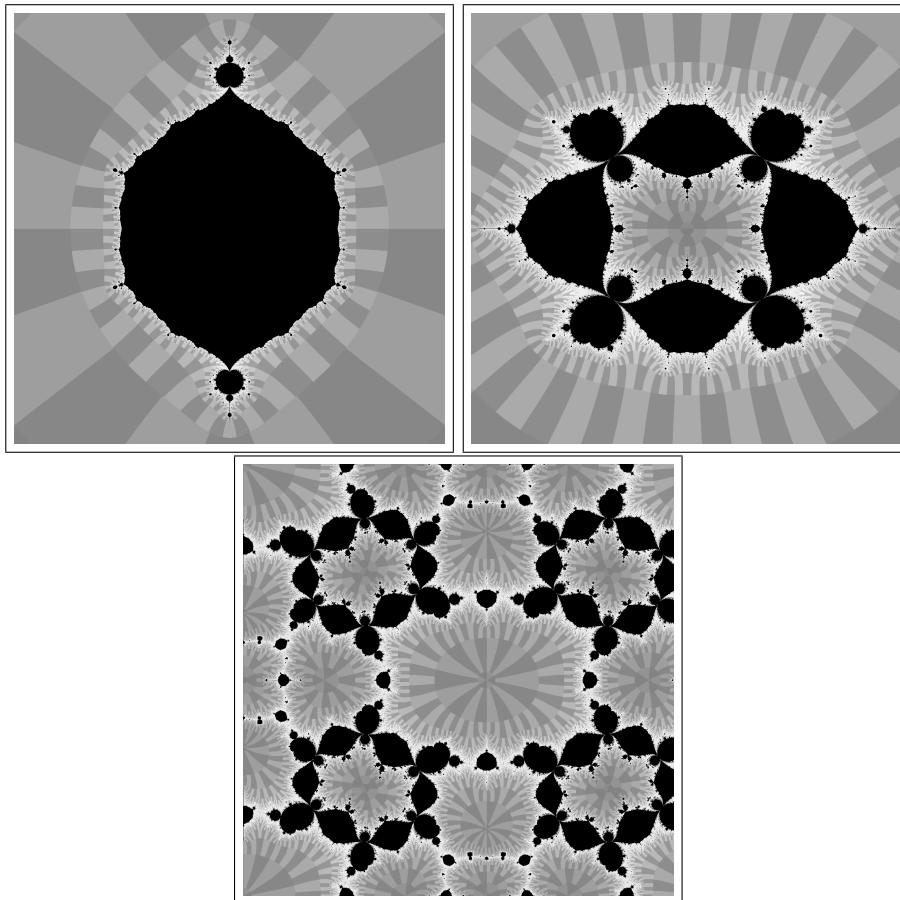


FIGURE 2. The superattracting curves \mathcal{S}_p for $p = 1, 2, 3$.

which has a period 3 critical orbit

$$0 \mapsto 1 \mapsto c \mapsto 0.$$

Similarly, to take a single branch of $\gamma = \sqrt{\alpha}$, we need to solve the following equation on (γ, c) :

$$(c^3 - c^2)\gamma^2 = -c^3 + c^2 - 1.$$

This equation is equivalent to

$$\left(\frac{2ic\gamma}{c-1}\right)^2 = 4p^3 - g_2p - g_3$$

where

$$(4) \quad p = \frac{1}{c-1} + \frac{1}{3}, \quad g_2 = -\frac{20}{3}, \quad g_3 = -\frac{44}{27}.$$

Therefore, \mathcal{S}_3 is a torus with punctures (indeed there are 8 punctures) and it can be parametrized using a Weierstrass \wp -function satisfying

$$(5) \quad (\wp')^2 = 4\wp^3 - g_2\wp - g_3.$$

By definition, \mathcal{S}_p ($p \geq 1$) are mutually disjoint. Furthermore, since $\text{supp } \mu_{\text{bif}} = \overline{\text{Mis}}$, it is also disjoint from \mathcal{S}_p .

Milnor [M2] proved that \mathcal{S}_p is a smooth affine curve for any $p \geq 1$. It is not known if \mathcal{S}_p is always connected (equivalently, irreducible). As p increases, the genus and the number of punctures of \mathcal{S}_p grows exponentially, so it gets more and more complicated rapidly.

The action of two involutions ι_{can} and ι_{cp} are as follows:

- Since ι_{can} preserves the property that the marked critical point is periodic of period p , $\iota_{\text{can}} : \mathcal{S}_p \rightarrow \mathcal{S}_p$ is a conformal automorphism on \mathcal{S}_p .
- The image $\mathcal{S}'_p = \iota_{\text{cp}}(\mathcal{S}_p)$ is the parameter set where the other critical point $-a$ is periodic of exact period p .

For $p, p' > 0$, the intersection $\mathcal{S}_p \cap \mathcal{S}'_{p'}$ corresponds to the set of parameters such that both a and $-a$ are periodic of period p and p' respectively. Milnor [M2] proved that \mathcal{S}_p and $\mathcal{S}'_{p'}$ intersect transversally for any $p, p' > 0$.

5. VISUALIZATION

5.1. Stereo Viewer. Stereo Viewer was developed by Ushiki [U] to see complex two-dimensional Julia sets. This program is divided into several parts: The main part is only for visualization and the user interface, and it calls other programs, calculating Julia sets and (un)stable manifolds for saddle fixed points, and outputting data files (DTS file).

A DTS file consists of coordinates and colors of points in real 4-dimensional space. Stereo Viewer reads up to five DTS files and projects the points in the DTS files into 3-dimensional space, and show with help of OpenGL, a commonly-used library for 2D and 3D graphics. One can dynamically rotate objects not only in the 3-dimensional space, but also in the 4-dimensional space. It is also possible to show (cross-eyed) stereogram to see sterically.

Remark 5.1. A sample code to make a DTS file in C programming is as follows:

- (1) First open a file:


```
sfile = fopen("filename.dts", "w");
```
- (2) Output the number of points to be contained in the file:


```
fwrite(&num, sizeof(int), 1, sfile);
```
- (3) Output the coordinates (of type float) and the color (of type unsigned int) for each point:


```
fwrite(&xre, sizeof(float), 1, sfile);
fwrite(&xim, sizeof(float), 1, sfile);
fwrite(&yre, sizeof(float), 1, sfile);
fwrite(&yim, sizeof(float), 1, sfile);
col = (alpha << 24) | (b << 16) | (g << 8) | r;
fwrite(&col, sizeof(unsigned int), 1, sfile);
```
- (4) Repeat (3) for all points.

The color format is RGBA, but it seems alpha channel (transparency) does not affect. If a point is sufficiently close to the real plane, then it is automatically colored in red.

Because of the endian and the size of the types (int, float, etc.), one might need to re-compile Stereo Viewer to work properly.

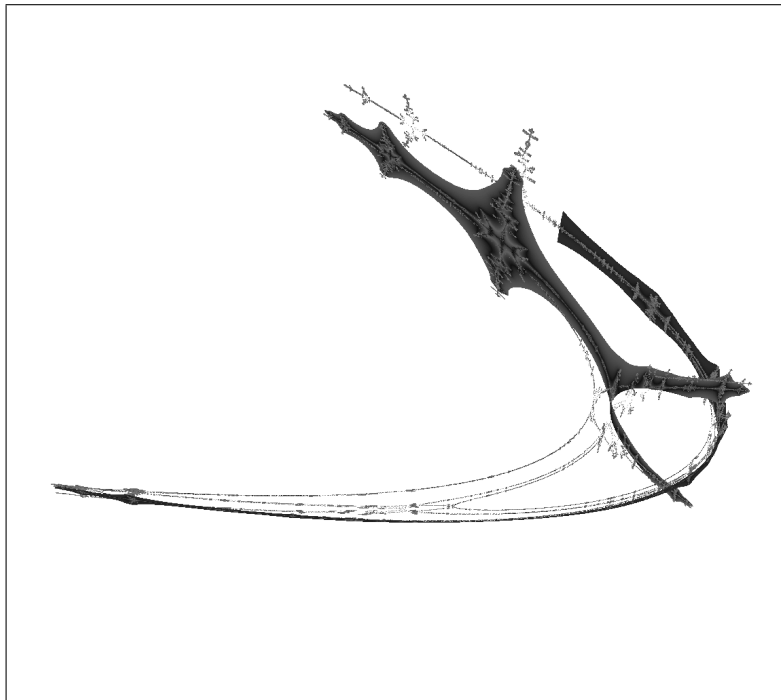


FIGURE 3. Stereo Viewer showing the Julia set and the unstable and stable manifolds of a saddle fixed points of Hénon map $H(x, y) = (x^2 - 1.4 + 0.3y, x)$.

5.2. Visualization of the bifurcation measure. We calculate the bifurcation measure with help of the landing theorem (Theorem 3.4). Namely, we compute the Goldberg map $\Phi_g(\Theta, r)$ for small $r > 0$. Let $\Theta = (\theta^+, \theta^-) \in \mathbf{Cb}_0 \subset (\mathbb{R}/\mathbb{Z})^2$ be a critical portrait. By using the fact that Böttcher coordinates are close to the identity near infinity, we can approximate $\Phi_g(\Theta, r)$ when r is large. First, observe that if $(a, b) = \Phi_g(\Theta, r)$, then we have $\varphi_{a,b}(f_{a,b}(\pm a)) = \exp(3r + 6\pi i\theta^\pm)$. Replacing $\varphi_{a,b}$ by the identity map, we get the following:

$$\begin{aligned} a^3 &= \frac{e^{3r}}{4}(e^{6\pi i\theta^-} - e^{6\pi i\theta^+}), \\ b &= \frac{e^{3r}}{2}(e^{6\pi i\theta^+} + e^{6\pi i\theta^-}). \end{aligned}$$

Now we need to choose a cubic root of a^3 appropriately. By a combinatorial assumption that $\theta^- \in (\theta^+ + \frac{1}{3}, \theta^+ + \frac{2}{3})$, we can take representatives $\theta^+, \theta^- \in \mathbb{R}$ satisfying $\theta^- - \theta^+ \in (\frac{1}{3}, \frac{2}{3})$. Then we have $6\pi(\theta^+ - \theta^-) \in (-4\pi, -2\pi)$, hence it follows that

$$\begin{aligned} \arg(a^3) &= \arg(e^{6\pi i\theta^-} (1 - e^{6\pi i(\theta^+ - \theta^-)})) \\ &= 6\pi\theta^- + \frac{1}{2}(6\pi(\theta^+ - \theta^-) + 4\pi) - \frac{\pi}{2} \\ &\equiv 3\pi(\theta^+ + \theta^-) - \frac{\pi}{2} \pmod{2\pi}. \end{aligned}$$

Therefore,

$$\begin{aligned}\arg a &\in \pi \left(\theta^+ + \theta^- - \frac{1}{6} \right) + \frac{2\pi}{3}\mathbb{Z} \\ &= 2\pi\theta^+ + \pi \left(\theta^- - \theta^+ - \frac{1}{6} \right) + \frac{2\pi}{3}\mathbb{Z}.\end{aligned}$$

Thus the argument of the marked cocritical point $-2a$ satisfies the following:

$$\begin{aligned}\frac{1}{2\pi} \arg(-2a) - \theta^+ &\in \frac{1}{2} + \frac{1}{2}(\theta^- - \theta^+) - \frac{1}{12} + \frac{1}{3}\mathbb{Z} \\ &\subset \left[\frac{7}{12}, \frac{9}{12} \right] + \frac{1}{3}\mathbb{Z} \\ &= \left(\left[\frac{7}{12}, \frac{9}{12} \right] \cup \left[-\frac{1}{12}, \frac{1}{12} \right] \cup \left[\frac{3}{12}, \frac{5}{12} \right] \right) + \mathbb{Z}.\end{aligned}$$

Therefore, in order to let $\arg(-2a)$ close to θ^+ , we get

$$\arg a = \pi \left(\theta^+ + \theta^- - \frac{1}{6} \right) + \frac{2\pi}{3} = \pi(\theta^+ + \theta^-) + \frac{\pi}{2}.$$

As a conclusion, when $r > 0$ is sufficiently large, then $\Phi_g(\Theta, r)$ is approximated by $f_{a,b}$ such that

$$(6) \quad a = \frac{e^r}{4^{\frac{1}{3}}}(e^{2\pi i\theta^-} - e^{2\pi i\theta^+}), \quad b = \frac{e^{3r}}{2}(e^{6\pi i\theta^+} + e^{6\pi i\theta^-}).$$

Now we let $r \searrow 0$. We repeatedly Newton's method in \mathbb{C}^2 to solve the following equations on (a, b) :

$$(7) \quad f_{a,b}^n(\pm a) = \exp(3^n r + 3^n \pi i \theta^\pm).$$

Fix $r_0 > 0$ sufficiently large. For each $\Theta \in \text{Cb}_0$, let (a_0, b_0) be the initial value defined by (6) for $r = r_0$. The algorithm is as follows. Let $\varepsilon > 0$ be sufficiently small.

- (1) Let $l = \log r_0$ and $(a, b) = (a_0, b_0)$.
- (2) Decrease l by ε (i.e., $l := l - \varepsilon$).
- (3) Take the smallest $n > 0$ which satisfy $3^n e^l \geq r_0$.
- (4) Solve the equation (7) by Newton's method with initial value (a, b) , and replace the variables (a, b) by the obtained solution.
- (5) Repeat (2)-(4) until n gets sufficiently large.

Figure 4 shows a picture of the bifurcation measure approximated by this algorithm. We also plotted the real part (i.e., the landing points for real stretching rays), which corresponds to the bifurcation locus in the second and fourth quadrants for the family of real cubic polynomials $z^3 - 3Az + \sqrt{B}$ (see Figure 5).

To execute Newton's method, we need the derivative $\frac{\partial}{\partial a}(f_{a,b}^n(\pm a))$. In most cases, this diverges exponentially fast, so indeed it is impossible to iterate so many times. We do the calculation until $n = 30$, but Newton's method already diverges for some $\Theta \in \text{Cb}_0$.

5.3. Visualization of superattracting curves. We can generally visualize any one-parameter family. Here we only treats \mathcal{S}_p , but one can apply similar method to any algebraic curve in \mathbb{C}^2 .

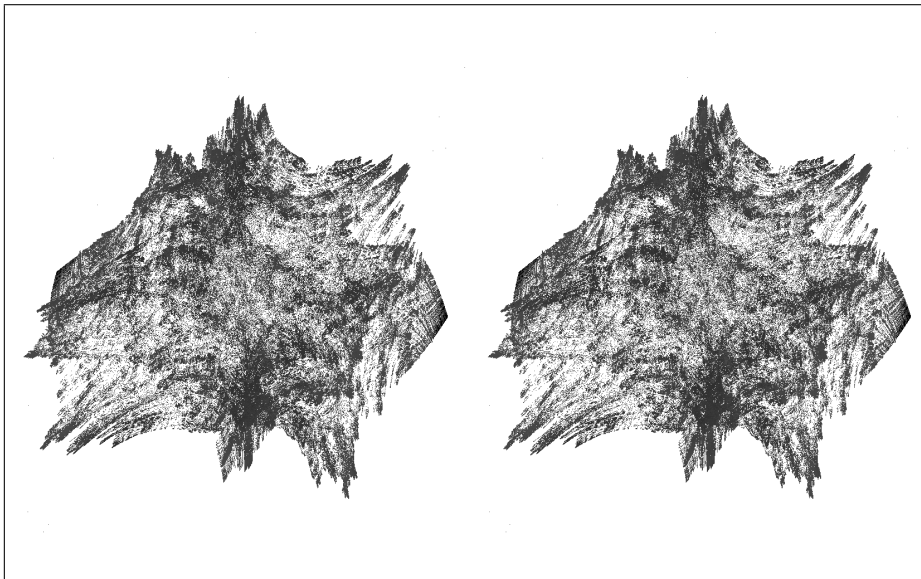


FIGURE 4. A stereoscopic image of the bifurcation measure μ_{bif} visualized by Stereo Viewer.

5.3.1. *Direct calculation for $p = 1, 2, 3$.* Since we know the exact parametrizations of \mathcal{S}_p for $p = 1, 2, 3$, we can use those to compute.

We would like to plot points in \mathcal{S}_p which is close to the bifurcation locus. The following algorithm is the simplest way to do this. To get a better approximation, one can apply Milnor's distance estimate algorithm to draw pictures of Julia sets [M1, Appendix H] for instance.

Let us assume \mathcal{S}_p is parametrized by $t \in \Omega \subset \mathbb{C}$.

- (1) Fix $R > 0$ sufficiently large, integers $N > N_0 > 0$, and a grid $\Gamma \subset \Omega$ (for example, $\Gamma = (\varepsilon\mathbb{Z} + \varepsilon i\mathbb{Z}) \cap \Omega$ for small ε).
- (2) For each $t \in \Gamma$, calculate the corresponding parameter $(a, b) \in \mathbb{C}^2$ and the orbit $\{f_{a,b}^n(-a)\}_{n=1,\dots,N}$ until it satisfies the escaping condition $|f_{a,b}^n(-a)| > R$. The smallest such n is called the *escaping time*.
- (3) Plot the point (a, b) with the color corresponding to n if $-a$ escapes to infinity and the escaping time n satisfies $N_0 \leq n \leq N$.

By definition, the marked critical point never escapes to infinity for $f_{a,b} \in \mathcal{S}_p$. Thus we only need to check the orbit of the other (free) critical point $-a$. For other curves, one might need to consider both of the critical points, so one need to plot when either one of the critical points, or both of the critical points escapes to infinity with the escaping time $N_0 \leq n \leq N$.

Figures 6–9 show the bifurcation loci of \mathcal{S}_p for $p = 1, 2, 3$, visualized by Stereo Viewer. By rotating dynamically on a computer, one can see how \mathcal{S}_p and $\mathcal{S}'_{p'}$ intersects for $p, p' \leq 2$. Although \mathcal{S}_3 is topologically just an eight-punctured torus, the picture looks too complicated to see how it is embedded into \mathbb{C}^2 .

Remark 5.2. To draw \mathcal{S}_3 , we also need to calculate a Weierstrass \wp -function. Coquereaux, Grossmann and Lautrup [CGL] gave a quite effective method to compute

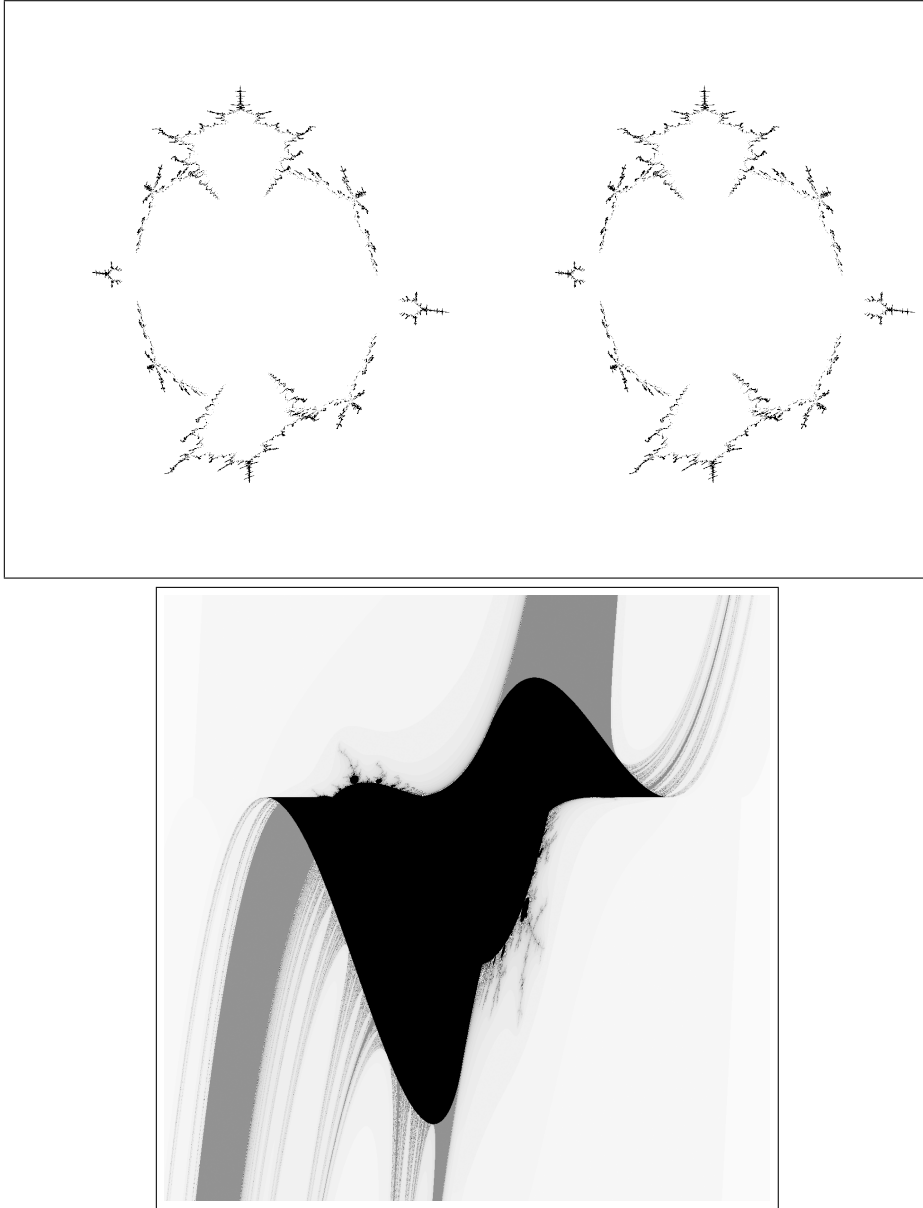


FIGURE 5. A stereoscopic image of the real part of the bifurcation measure and the family of real cubic polynomials $z^3 - 3Az + \sqrt{B}$.

the \wp -function defined by the differential equation (5). Their method is iterative; they use the duplication formula

$$\wp(2z) = -2\wp(z) + \frac{[6\wp^3(z) - \frac{1}{2}g_2]^2}{4[4\wp^3(z) - g_2\wp(z) - g_3]}$$

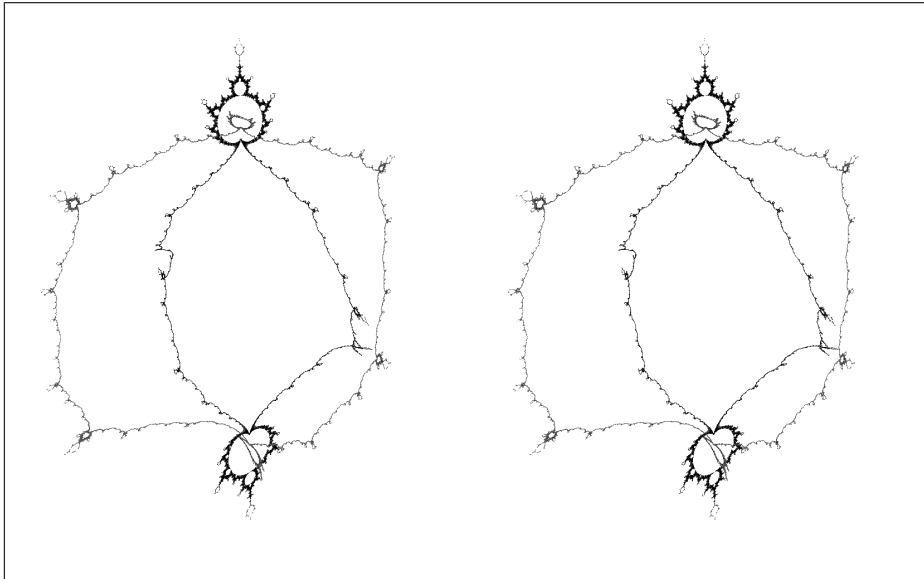


FIGURE 6. The bifurcation loci of \mathcal{S}_1 and \mathcal{S}'_1 embedded in \mathbb{C}^2 . Compare Figure 2.

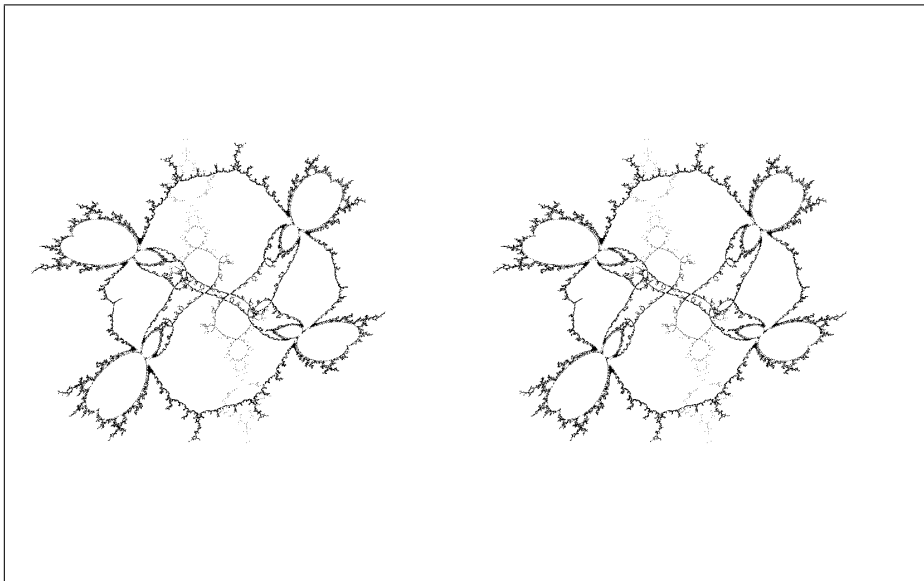


FIGURE 7. The bifurcation loci of \mathcal{S}_2 embedded in \mathbb{C}^2 . Compare Figure 2.

and the Laurent expansion near the origin. Moreover, they also give an iterative way to compute the periods for given g_2 and g_3 .

An implementation of their method is included in the source code of QFract which is available from the author's website.

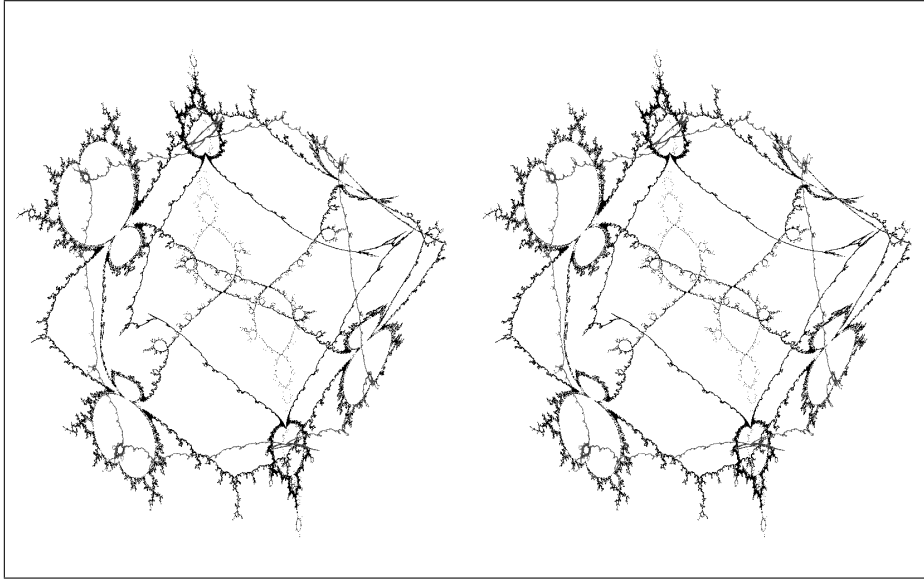


FIGURE 8. The bifurcation loci of \mathcal{S}_1 , \mathcal{S}'_1 and \mathcal{S}_2 embedded in \mathbb{C}^2 . Compare Figure 2.

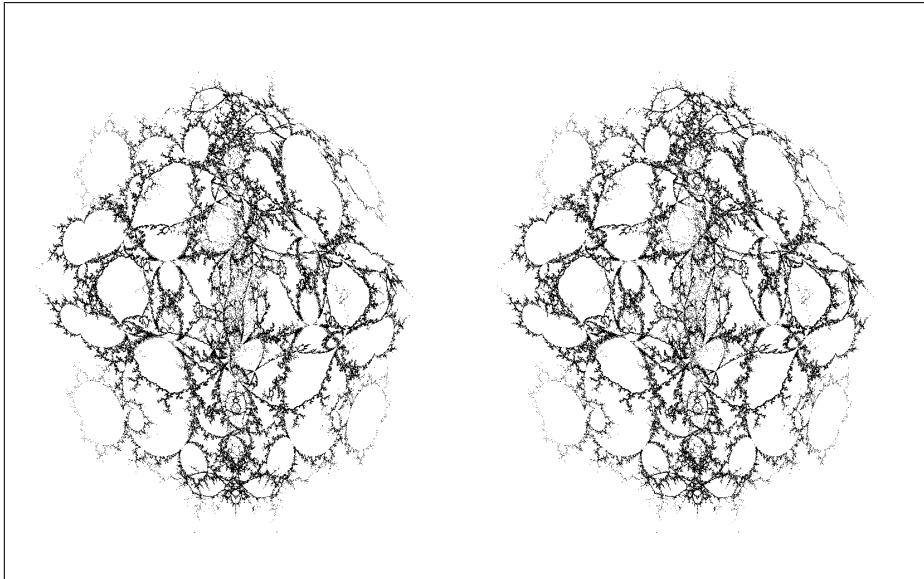


FIGURE 9. The bifurcation locus of \mathcal{S}_3 embedded in \mathbb{C}^2 . Compare Figure 2.

For \mathcal{S}_3 , the constants g_2 and g_3 are given in (4). A numerical computation shows that the periods are given by the following:

$$A = 3.410\dots, \quad B = 1.705\dots + 1.509\dots i.$$

5.3.2. *Solving Hamiltonian dynamics.* Even when we have a direct parametrization for a given smooth affine curve in \mathbb{C}^2 , one can get a local holomorphic coordinate using Hamiltonian dynamics. See [AC] and [BKM] for more details. Hence we can similarly draw any curve if one can calculate the defining equation and its derivatives.

We have not yet implemented this method, because \mathcal{S}_3 is already too complicated. It seems we need to develop a better user interface first to understand \mathcal{S}_p for $p \geq 4$ (cf. Section 7).

6. QUADRATIC RATIONAL FAMILY

Although we gave the definition of the bifurcation measure only for the cubic polynomial family, it is defined not only for any degree at least two, but also (in fact, originally) for the family of rational maps (see [BB] and [DF]). However, we do not know how to compute the bifurcation measure, neither Misiurewicz parameters.

On the other hand, one can similarly draw one-parameter families for the quadratic rational family, which is essentially of complex dimension two.

Figure 10 shows complex one-dimensional picture of \mathcal{S}_p for $p = 2, 3, 4$. Figures 11–13 show those curves under the parametrization $f_{a,b}(z) = \frac{z^2+a}{z^2+b}$. Observe that the critical points for $f_{a,b}$ are 0 and ∞ . We regard ∞ as the marked critical point and similarly define curves superattractive curves \mathcal{S}_p ($p \geq 1$).

$p = 1$: \mathcal{S}_1 is just the well-known Mandelbrot set. Since we always have $f_{a,b}(\infty) = 1$, the curve \mathcal{S}_1 indeed lie in the line at infinity of this parameter space. The involuted image $\mathcal{S}'_1 = \iota_{\text{cp}}(\mathcal{S}_1)$ is equal to a line $\{b = 0\}$.

$p = 2$: We have $\mathcal{S}_2 = \{f_{a,b}(1) = \infty\} = \{a = -1\}$ is a line and $\mathcal{S}'_2 = \{f_{a,b}(\frac{a}{b}) = 0\} \setminus \mathcal{S}'_1 = \{a = b^2\}$.

$p = 3$: For $f_{a,b} \in \mathcal{S}_3$, let $t = f_{a,b}(1) = f_{a,b}^2(\infty)$. Then we have $f_{a,b}(t) = \infty$, hence it follows that

$$\mathcal{S}_3 = \{(1 - t^2)t - 1, -t^2\} \in \mathbb{C}^2.$$

$p = 4$: Let us take a Möbius conjugacy for $f_{a,b} \in \mathcal{S}_4$ such that $\infty \xrightarrow{2} 0 \mapsto 1 \mapsto s \mapsto \infty$. Then it must have the following form:

$$z \mapsto \frac{s(s-1)}{(z-s)((s-2)z+1-s)}.$$

See Figure 10. Note that since the bifurcation locus for \mathcal{S}_4 is unbounded in the s -plane, a Möbius coordinate change is applied to get a bounded picture.

7. PROBLEMS AND FURTHER IMPROVEMENTS

Here, we summarize problems and further possibility for improvements.

7.1. The case of the Mandelbrot set. First of all, to see how accurate our picture is (or isn't), we show a picture of the Mandelbrot set drawn with the same algorithm in Figure 14.

Clearly it is quite rough, compared to any reasonable picture of the Mandelbrot set we can get nowadays. Especially near parabolic parameters, we need much more iteration and density to get detailed picture.

Hence, unfortunately, we do not have any nice mathematical suggestion which can be read from those pictures. In the following, we discuss how one can improve those pictures for better understanding.

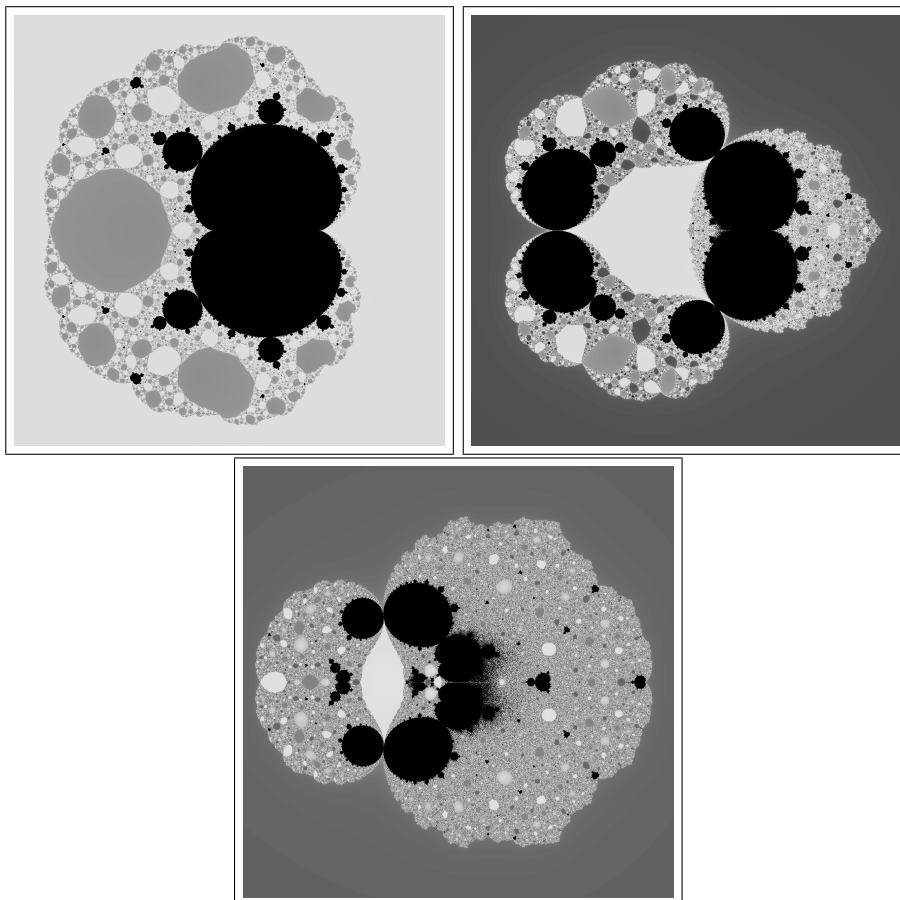


FIGURE 10. The superattracting curves \mathcal{S}_p ($p = 2, 3, 4$) for the quadratic rational family.

7.2. More iteration. As we have already mentioned in Section 5.2, derivatives rapidly diverges to infinity as the number of iteration increases. That prevents to solve the equation (7) by Newton's method.

For example, as in the case of the Mandelbrot set, we need more iteration if a stretching ray of critical portrait $\Theta \in \text{Cb}_0$ lands (or accumulates) at a parameter (a^*, b^*) having a parabolic periodic point. Say the marked critical point a^* is in the parabolic basin for f_{a^*, b^*} . However, if we further assume that $-a^*$ is preperiodic and repelling for f_{a^*, b^*} , then the derivative along the orbit of $-a$ grows exponentially for (a, b) close to (a^*, b^*) . Therefore, Newton's method diverges and we cannot very get close to (a^*, b^*) .

7.3. Subdivision. To visualize the bifurcation measure, it is reasonable to take an equidistributed grid in $\text{Cb}_0 \subset (\mathbb{R}/\mathbb{Z})^2$. However, to get a nice picture of its support $\overline{\text{Mis}}$, it is better to let points equidistributed in the parameter space \mathbb{C}^2 (this is suggested by Thurston).

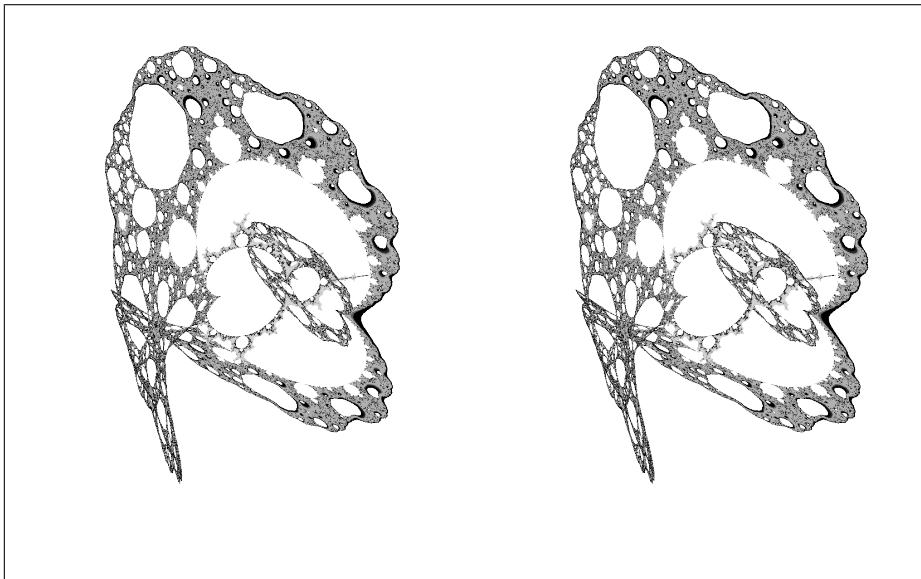


FIGURE 11. Superattracting curves \mathcal{S}'_1 , \mathcal{S}_2 and \mathcal{S}'_2 for quadratic rational family.

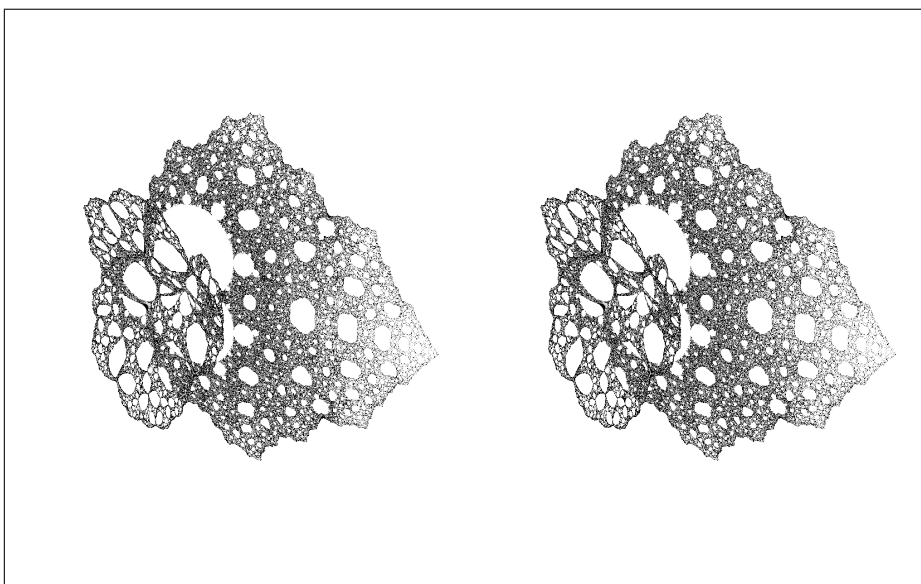


FIGURE 12. Superattracting curve \mathcal{S}_3 for quadratic rational family.

In order to do that, we need to change the density in Cb_0 depending on the Jacobian matrix of the landing map $e : \text{Cb} \rightarrow \mathcal{C}$, or $\Phi_g(\cdot, r) : \text{Cb}_0 \rightarrow \mathbb{C}^2$ for small $r > 0$. Hence we need to use some algorithm to dynamically subdivide Cb_0 .

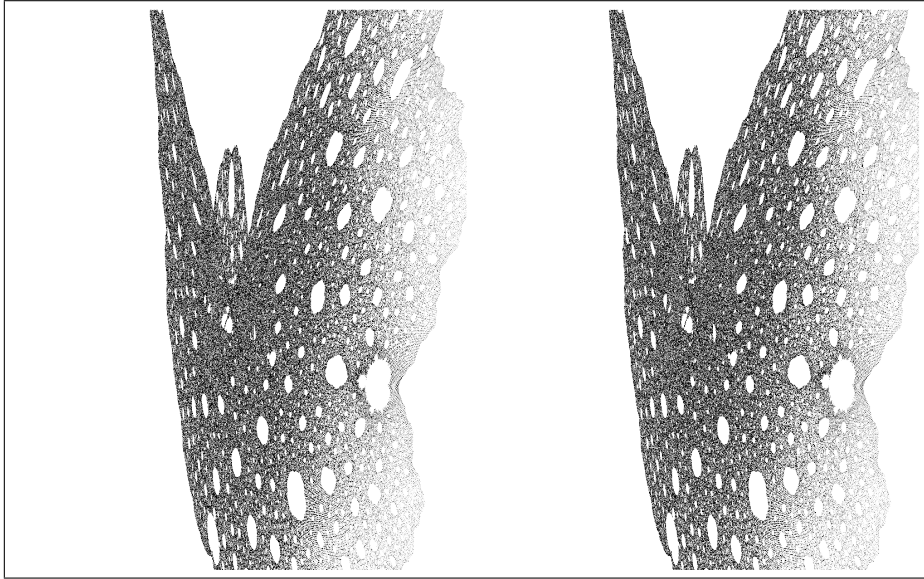


FIGURE 13. Superattracting curves \mathcal{S}_4 for quadratic rational family.

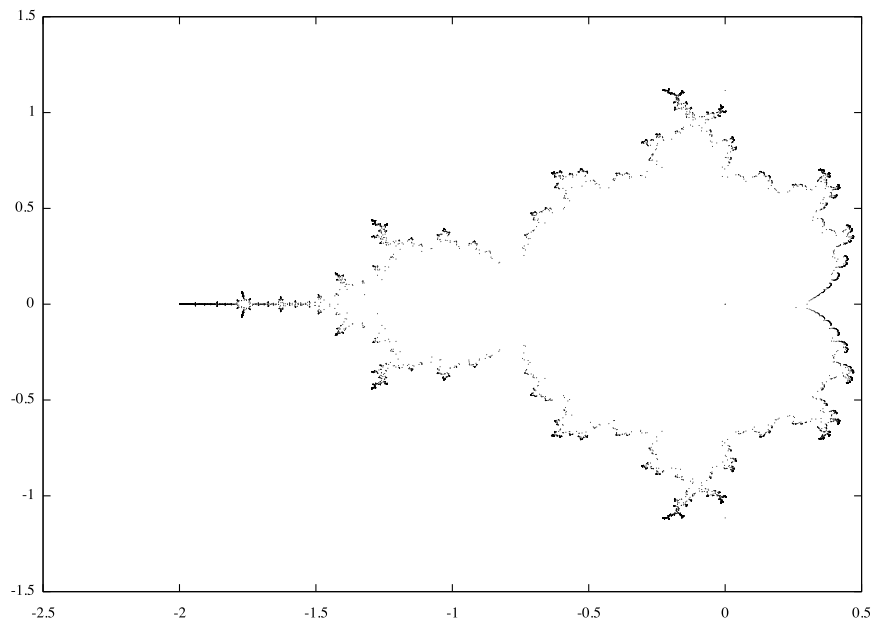


FIGURE 14. Bifurcation measure for the quadratic family.

This type of subdivision method should be also useful for one-parameter families. We took equidistributed grids in the parameter spaces of the curves. Hence the density in Stereo Viewer varies depending on derivatives of embeddings. Some part

looks very small in the one-parameter family but it can be large in \mathbb{C}^2 (compare Figure 2 and Figures 6-9).

7.4. The bifurcation measure for the quadratic rational family. As already mentioned, we do not know how to compute the bifurcation measure, nor Misiurewicz parameters (with high (pre)periods) for the family of quadratic rational maps. One might need to find a non-rigorous method to find Misiurewicz parameter in a reasonable time like Biham-Wenzel's method.

7.5. Better user interface. A good graphical user interface (GUI) plays an important role to see many phenomena from pictures. The following is a list of some nice functionalities implemented some programs drawing the Mandelbrot set, Julia sets and so on:

Zooming: One can zoom in any part of the picture.

Dynamically drawing Julia sets: If one click (or double-click) the parameter space, then the corresponding Julia set is shown.

Forward and backward orbit: One can see the forward/backward orbits of the pointed point in the phase space. Some programs can even draw orbits of the set of many points to see the forward/backward images of a curve, and so on.

As we see in Section 5.3, the embedded \mathcal{S}_p is already too complicated to see in Stereo Viewer when $p = 3$. Zooming feature looks necessary to see such knotty objects. Since the space is real four-dimensional, we might need not only zooming, but also moving and rotating around the whole space with help of keyboard or joystick.

Then it might be helpful to add a functionality to dynamically show the Julia set of the parameter at the center of the picture (it looks difficult to implement an user interface to pick a parameter in \mathbb{C}^2), to see what happens in the dynamical space. Drawing one-parameter families orthogonal to the screen might be also informative.

REFERENCES

- [AC] D. A. Aruliah and R. M. Corless. *Numerical parameterization of affine varieties using ODEs*. International Conference on Symbolic and Algebraic Computation. Proceedings 2004 International Symposium on Symbolic and Algebraic Computation, Santander, Spain, 2004, 12–18.
- [BB] G. Bassanelli, F. Berteloot. *Bifurcation currents in holomorphic dynamics on \mathbb{P}^k* . J. Reine Angew. Math. 608 (2007), 201–235.
- [BH] B. Branner, J. H. Hubbard. *The iteration of cubic polynomials. I. The global topology of parameter space*. Acta Math. 160 (1988), 143–206.
- [BKM] A. Bonifant, J. Kiwi and J. Milnor. *Cubic Polynomial Maps with Periodic Critical Orbit, Part II: Escape Regions*. Conform. Geom. Dyn. 14 (2010), 68–112.
- [CGL] R. Coquereaux, A. Grossmann and B. E. Lautrup. *Iterative Method for Calculation of the Weierstrass Elliptic Function*. IMA J. Numer. Anal. 10 (1990), 119–128.
- [DM] L. DeMarco. *Dynamics of rational maps: a current on the bifurcation locus*. Math. Res. Lett. 8 (2001), 57–66.
- [DF] R. Dujardin, C. Favre. *Distribution of rational maps with a preperiodic critical point*. Amer. J. Math. 130 (2008), 979–1032.
- [DMS] M. J. Davis, R. S. MacKay, A. Sannami. *Markov shifts in the Hénon family*. Physica D 52 (1991), 171–178.
- [G] L. R. Goldberg. *On the multiplier of a repelling fixed point*. Invent. Math. 118 (1994), 85–108.

- [KN] Y. Komori, S. Nakane. *Landing property of stretching rays for real cubic polynomials*. Conform. Geom. Dyn. 8 (2004), 87–114.
- [M1] J. Milnor. *Dynamics in one complex variable*. Third edition. Annals of Mathematics Studies, 160. Princeton University Press, Princeton, NJ, 2006.
- [M2] J. Milnor. *Cubic Polynomial Maps with Periodic Critical Orbit, Part I*. Complex dynamics, 333–411, A K Peters, Wellesley, MA, 2009.
- [U] S. Ushiki. Stereo Viewer. <http://www.math.h.kyoto-u.ac.jp/~ushiki/>

DEPARTMENT OF MATHEMATICS, KYOTO UNIVERSITY.
URL: <http://www.math.kyoto-u.ac.jp/~inou/>